Cellulose (2009) 16:1–8
DOI 10.1007/s10570-008-9252-2

Varietal difference in cellulose microfibril dimensions observed by infrared spectroscopy

Yoshiki Horikawa · Bruno Clair · Junji Sugiyama

Received: 27 December 2007 / Accepted: 5 September 2008 / Published online: 25 September 2008

Abstract We have previously reported a novel Fourier transform infrared (FTIR) method for evaluating both the accessibility and lateral dimensions of cellulose microfibrils. This method differs from conventional deuteration in that the OH groups in the crystalline region were initially completely deuterated. The samples were then rehydrogenated by immersing them in water at 25 °C, during which only the OD groups on the surface were rehydrogenated. The ratio of OD to OH groups measured for cellulose from various origins was used to estimate microfibril dimensions, which were compared with the data from X-ray diffractometry. The rehydrogenation process was further investigated by immersing the deuterated samples in water at elevated temperatures. The behavior of rehydrogenation under heat treatment was converted to observe the microfibril shape, which was in good agreement with the cross-sectional images obtained by diffraction contrast transmission electron microscopy techniques.

Y. Horikawa (✉) · J. Sugiyama
Research Institute for Sustainable Humanosphere,
Kyoto University, Uji, Kyoto 611-0011, Japan
e-mail: yhorikawa@rish.kyoto-u.ac.jp

B. Clair
Laboratoire de Mecanique et Génié Civil (LMGC), UMR 5508, CNRS, Université Montpellier 2, Place E. Bataillon, cc 048, Montpellier Cedex 5 34095, France

Keywords Deuteration · Rehydrogenation · Fourier transform infrared (FTIR) · Cellulose microfibril lateral dimension · Diffraction contrast imaging

Introduction

Cellulose is the most abundant biological polymer on earth and is the major component of cell walls in higher plants, as well as in some algae. Cellulose-synthesizing organisms are widely distributed in all biological kingdoms, ranging from bacteria to higher plants and tunicates. Cellulose of different origins has been analyzed with respect to various microfibril features, including microfibril size, cross-sectional shape, allomorphism, and uniplanar orientation behavior. Microfibril size has been characterized by transmission electron microscopy (TEM) and X-ray analysis, and it is estimated to be approximately 3 nm in higher plants and, generally, considerably larger in marine algae and tunicates.

In a previous report (Horikawa and Sugiyama 2008), the accessibility of *Valonia* cellulose microcrystals, whose ultrastructure was well characterized (Sugiyama et al. 1984, 1985), was investigated by combined deuteration/rehydrogenation and Fourier transform infrared (FTIR) spectroscopy. This method is similar to the classical deuteration technique for estimating the accessibility of cellulosics; however, a

novel aspect of the method is that the primary hydrogen groups are initially completely deuterated. The deuterated samples were then rehydrogenated by immersing them in water at 25 °C—the temperature at which all surface OD groups are substituted with OH groups. The accessibility ratio was in good agreement with the surface/core ratio calculated from the 33 × 38 β-(1,4)-homoglucan chains in *Valonia* cellulose microfibrils (Sugiyama et al. 1985). We proposed that the accessibility of the cellulose microcrystal surface can be used to estimate the microfibril dimensions. In addition to accessibility at 25 °C, the behavior during rehydrogenation at elevated temperatures conferred accessibility to the crystal core. This process might be related to the structural properties of cellulose microfibrils independent of their dimensions.

The aim of this study was to apply the abovementioned technique to examine the cellulose microfibrils produced by various higher plants, algae, and tunicates. We performed rehydrogenation at 25 °C for measuring the microfibril dimensions by FTIR, and further investigated the process of accessibility at elevated temperatures in order to estimate the microfibril shape. The results obtained were compared with electron microscopic images. On the basis of our observations, we discuss the suitability of this method for evaluating microfibril structure.

Material and methods

Cellulose samples

Valonia ventricosa was obtained from Florida Keys, USA. The specimens were purified by boiling them in 1% NaOH for 10 h. Then, they were thoroughly rinsed with distilled water before being soaked overnight in 0.05 N HCl at room temperature. The following day, the specimens underwent bleaching treatment for 2 h at 70 °C in 0.3% $NaClO_2$, buffered at a pH of 4.9 with acetate buffer. This treatment was repeated until an infrared band at 1,600 cm^{-1}, which was assigned to the carbonyl group, disappeared completely. Following this, the samples were soaked in 5% KOH overnight and washed in distilled water.

Halocynthia roretzi and *Ciona intestinalis* were initially treated overnight with 5% KOH at room temperature and then rinsed in distilled water until neutrality was achieved. The samples were then treated at 70 °C for 2 h with a bleaching solution. The entire treatment was repeated several times until the noncellulosic contaminants were completely eliminated.

A strain of *Micrasterias crux-melitensis* (IAM-C-427) was supplied from the culture collection of the Institute of Molecular and Cellular Research, the University of Tokyo. The samples were boiled in 1% NaOH for 8 h and then washed with distilled water. They were then treated at 70 °C for 2 h in a bleaching solvent. This bleaching treatment was followed by thorough washing and overnight dispersion into 5% KOH. These bleach and 5% KOH treatments were repeated several times until the sample was completely purified, which was determined by FTIR.

Picea sitkensis was a gift from M. Norimoto, Doshisha University. *Populus maximowiczii*, including its G-fiber and normal wood, was obtained from our wood collection. Thin longitudinal slices from these wood blocks were treated with 50% HNO_3 and 6% $KClO_3$ (Schultz's solution) at 60 °C for 1 h along with continuous stirring. The products were then thoroughly washed with distilled water in order to achieve neutrality.

Cotton linter was supplied by Asahi Kasei Corporation, and the other purified cellulose samples, such as cotton, bagasse, Ecuador abaca, straw, bamboo, kenaf fiber, and Philippine abaca, were a gift from Toho Tokushu Pulp Co. Ltd.

Deuteration and rehydrogenation

With the exception of cellulose samples from higher plants, all other samples were subjected to annealing in D_2O for 1 h at 260 °C, during which all the OH groups involved in hydrogen bonding were replaced by deuterium atoms. When higher plant samples were deuterated at this temperature, the fiber morphology became markedly degraded. Therefore, intracrystalline deuteration (Nishiyama et al. 1999) of these samples was performed by annealing them in 0.1 N NaOD/D_2O for 1.5 h at 190 °C. Perfect conversion from OH to OD was confirmed by washing the deuterated celluloses in 0.1 N NaOH at 185 °C—the temperature at which all OD bonds reverted to OH bonds, as determined by the FTIR spectra. After complete deuteration, the samples were immersed in

water and rehydrogenated at elevated temperatures for 1 h.

FTIR spectroscopy

Two modes of FTIR were employed, namely, the microscopic and ATR (attenuated total reflection)-FTIR techniques. In the former, the instrument was equipped with a low-noise detector (HgCdTe) cooled at −196 °C. A drop of suspension was spotted on a BaF_2 crystal and subjected to FTIR measurement. A spectrum one FTIR spectrophotometer was used to measure the absorbance in the range of 4,000–700 cm^{-1} with a resolution of 4 cm^{-1} and 128 × integration. In the latter, the freeze-dried specimens were cut into approximately 1-cm squares, and then placed on a single reflection diamond ATR crystal top plate. The spectra were obtained in the range of 4,000–400 cm^{-1} with a resolution of 4 cm^{-1} and an acquisition of 128 scans.

X-ray diffractometry

X-ray diffractometry was performed in the transmission mode using Cu-K_α radiation generated from UltraX 18HF (Rigaku Corporation) operating at 30 kV and 100 mA ($\lambda = 0.1542$ Å). Peak separation of cellulose at (1–10), (110), (012), and (200) was carried out by least-square fitting by assigning Gaussian functions.

Diffraction contrast imaging with TEM

The samples were dehydrated with an ethanol or acetone series and subjected to propylene oxide as a substituting agent. The samples were then embedded in epoxy resin, and ultrathin sections of approximately 60 nm thickness were prepared using a diamond knife.

Observations were made using a JEM-2000EXII transmission electron microscope (JEOL Co. Ltd.) operating at 100 kV. The minimum dose system (MDS; JEOL Co. Ltd.) was used for diffraction contrast imaging in order to eliminate specimen damage caused by electron irradiation. A 100-μm objective aperture was inserted to eliminate all the diffracted beams from the crystalline regions; this enabled us to visualize the objects as dark contrast areas in the positive images. The images were recorded at a 10,000× magnification on a Mitsubishi MEM film.

Results and discussion

Rehydrogenation at 25 °C for the estimation of microfibril dimension

Figure 1 shows the five spectra that were recorded for *H. roretzi*, *M. crux-melitensis*, cotton linter, cotton, and bamboo cellulose after deuteration followed by rehydrogenation at 25 °C (Fig. 1a–e, respectively). When the cellulose microfibrils were completely deuterated, all the OH groups forming the hydrogen bond were exchanged with deuterium atoms. When the deuterated microfibrils are immersed in water at room temperature, only the surface moieties of the ODs come into contact with water since the remaining portion of the group lies buried within the core of the crystalline domain. In the spectra for *H. roretzi* and *M. crux-melitensis*, almost all the sharp OH stretching bands disappeared and were transferred to the OD stretching region as a result of deuteration (Fig. 1a and b). On the other hand, the OH

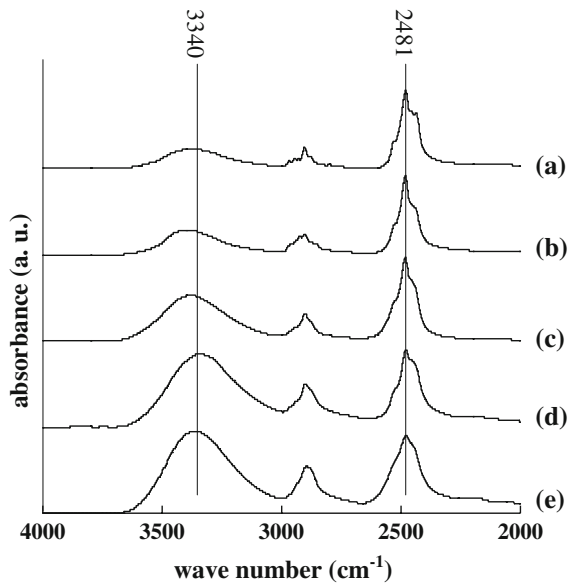

Fig. 1 FTIR spectra of H. roretzi, M. crux-melitensis, cotton linter, cotton, and bamboo cellulose rehydrogenated at 25 °C after deuteration (**a**–**e**, respectively). The bands at 3,340 and 2,481 cm^{-1} were ascribed to O-3-H···O-5 and O-3-D···O-5, respectively

absorbances of bamboo cellulose, the microcrystal structure of which is considerably smaller than that of tunicates or algae, were clearly discernable (Fig. 1e). Despite their similar origin, cotton linter is known to have higher crystallinity than normal cotton fiber. Moreover, in Fig. 1c and d, it is indeed possible to discern the difference between cotton linter and normal cotton fiber on the basis of their respective spectra.

OH and OD stretching bands were used to quantify the degree of hydrogen recovery, which is considered to be a measure of the accessibility of hydrogen to the crystal surface. The ratio of absorbance A at OH and OD indicates the remaining portion (R) of OD; R is obtained using the following equation:

$$R = A_{OD}/(A_{OH} + A_{OD})$$

Cellulose microfibrils are crystallized by intrahydrogen and interhydrogen bonds. All the infrared (IR) bands with O–H stretching vibration in the alcoholic groups appeared in the range of 3,600–3,000 cm^{-1}. Generally, the sharpest band (3,340 cm^{-1}) is assigned to the intrahydrogen bond O-3-H···O-5 (Maréchal and Chanzy 2000), and that at 2,484 cm^{-1} is likely to represent an O-3-D···O-5 bond. The height of these two bands was used for estimating the R value. It is considered that rehydrogenation at 25 °C could separate the microfibril surface from the remainder of the molecular chains, and that the R value is useful as an index of microfibril size. To confirm this assumption, the crystalline characterization of various cellulose samples was analyzed by X-ray diffractometry and represented in Table 1 as the full width at half maximum (FWHM) of the peak (200). As observed in Fig. 2, the R value at 25 °C is highly correlated with the FWHM of the (200) peak. Accordingly, the R value at 25 °C may be used to evaluate cellulose microfibril dimensions or crystalline perfection. However, three samples—*M. crux-melitensis*, *P. maximowiczii* normal wood, and *P. sitkensis*—were not located along the linear regression line. This departure observed for the cellulose of the two higher plants may be attributable to unpurified samples used for the X-ray analysis. With regard to *M. crux-melitensis*, since the cellulose microfibrils were mainly orientated in the (110) plane parallel to the plasma membrane (Kim et al. 1996; Koyama et al. 1997), it was considered not to characterize the microfibril on the basis of Bragg reflection of (200).

Table 1 R values at 25 °C and the full width at half maximum (FWHM) of the peak (200) on the basis of X-ray diffractometry

	FWHM (200) (degrees)	R value at 25 °C
V. ventricosa	0.535	0.934
H. roretzi	0.555	0.877
C. intestinalis	0.616	0.851
M. crux-melitensis	0.871	0.792
Cotton linter	0.685	0.664
P. maximowiczii tension wood	0.783 (untreated sample)	0.553
Bagasse	0.838	0.510
Cotton	0.710	0.507
P. maximowiczii normal wood	1.234 (untreated sample)	0.474
Ecuador abaca	0.893	0.463
Straw	0.902	0.461
Bamboo	0.877	0.438
Kenaf fiber	0.775	0.433
Phillipine abaca	0.890	0.418
P. sitkensis	1.275 (untreated sample)	0.396

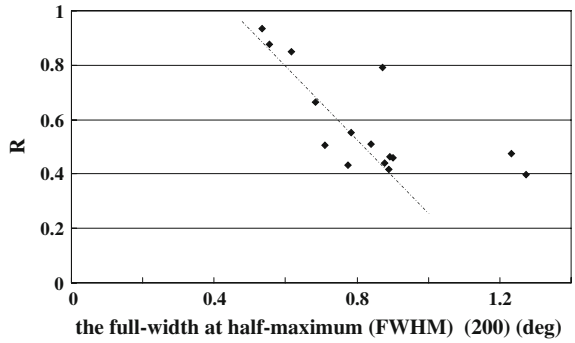

Fig. 2 Relationship between the R values at 25 °C and the half-width values of the (200) peak listed in Table 1. The regression line was obtained from all the samples except for the samples of P. maximowiczii normal wood, P. sitkensis, and M. crux-melitensis

Rehydrogenation at elevated temperatures for estimating microfibril shape

When deuterated cellulose samples from seven different origins were washed in water at an elevated temperature, all the R values decreased (Fig. 3). With regard to *V. ventricosa*, the depth of hydrogen penetration was essentially unaltered by an increase in temperature till 120 °C. With further heating,

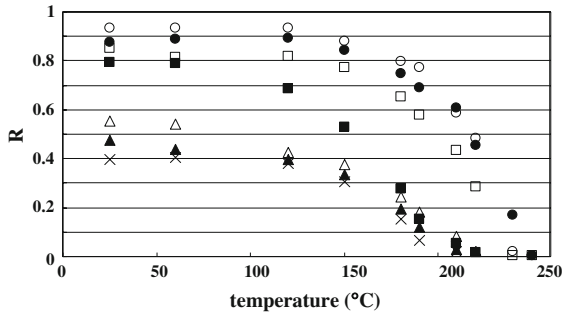

Fig. 3 The change in the *R* value of several cellulose samples at elevated temperatures. The ratio of absorbance *A* at OH and OD represents the OD remaining (*R*) in each sample; the *R* value was calculated using the following equation: $R = A_{OD}/(A_{OH} + A_{OD})$. ○, V. ventricosa; ●, H. roretzi; □, C. intestinalis; ■, M. crux-melitensis; Δ, P. maximowiczii tension wood; ▲, P. maximowiczii opposite site; ×, P. sitkensis

accessibility to the crystal core began to increase, and at approximately 220 °C, hydrogen rapidly penetrated into the crystal. This rapid penetration may correspond to the crystalline phase transition, which was recently reported in an X-ray diffraction study (Wada 2002). Finally, all the OD bonds were replaced with OH bonds rehydrogenated at 250 °C. Tunicates and *V. ventricosa* exhibit a similar curve pattern with respect to the temperature of initial hydrogen penetration and the rapid rehydrogenation. The *R* value for *H. roretzi* at each temperature was higher than that for *C. intestinalis*, indicating that the microfibrils of the former are larger than those of the latter. On the other hand, the *R* values of higher plants were very low compared to those for the tunicates and algae. Moreover, the exchange rate increased at approximately 180 °C, and these *R* values subsequently reached 0 at rehydrogenation temperatures below 220 °C. This shift to lower rehydrogenation temperatures in higher plants is thought to be attributable to the fact that the microfibril dimensions in these plants are considerably smaller than those in *V. ventricosa*. During rehydrogenation at each temperature, the *R* value of *P. maximowiczii* tension wood was higher than that of *P. maximowiczii* normal wood and *P. sitkensis*. Furthermore, when these higher plants samples were rehydrogenated at 210 °C, the OD bonds of *P. maximowiczii* normal wood and *P. sitkensis* were completely substituted with OH bonds, whereas incomplete substitution was observed in *P. maximowiczii* tension wood. These results appear to support the conventional opinion that the microfibril dimensions of G-fiber are larger than those of normal wood (Washusen and Evans 2001; Ruelle et al. 2007). However, the difference is so small that it could be interpreted as an enhanced disorder in the surface molecular chains of normal wood as a result of interaction between other cell wall components during lignification. In contrast, *M. crux-melitensis* displayed a unique trend that was clearly manifested suddenly at approximately 150 °C; this trend was not observed in tunicate samples that had a similar value at this temperature when rehydrogenated at 25 °C. These data indicate that the microfibrils of *M. crux-melitensis* are large and thin, that is, they exhibit a flatter shape. Moreover, rehydrogenation in *M. crux-melitensis* was completed at similar temperatures to that in *Populus* tension wood. This correspondence is instructive with respect to cellulose-synthesizing enzyme complexes, referred to as terminal complexes (TCs). The cellulose of almost all higher plants is believed to be synthesized by rosette-type TCs (Mueller and Brown 1980; Kimura et al. 1999). Similarly, the cellulose microfibrils in *Micrasterias*, belonging to the Zygnematales, are generated with a ribbon-like morphology by a hexagonal array of rosette-type TCs (Giddings et al. 1980). The variation in ribbon width is related to the number of individual rosettes, which contribute to microfibril formation, although the thickness is likely to be constant. Therefore, the similar accessibility to the crystalline core in both *M. crux-melitensis* and *P. maximowiczii* tension wood suggests a similar microfibril thickness in the Zygnematales and higher plants.

Comparison of data obtained by electron microscopy

In order to complement the results presented in Fig. 3, typical diffraction contrast images from ultrathin cross-sections were obtained by TEM (Fig. 4). This technique yielded diffraction contrast images of each of the microfibril cross-sections (Revol 1982). The shape of the *V. ventricosa* microfibril in cross-section, which included more than 1,000 molecular chains (Sugiyama et al. 1985), was almost square and the largest of all the samples examined. With respect to the unique microfibril cross-sectional structure in tunicates, Van Daele et al. (1992) observed that parallelogram- or diamond-shaped microfibrils were deposited in the tunic. Furthermore, Helbert et al.

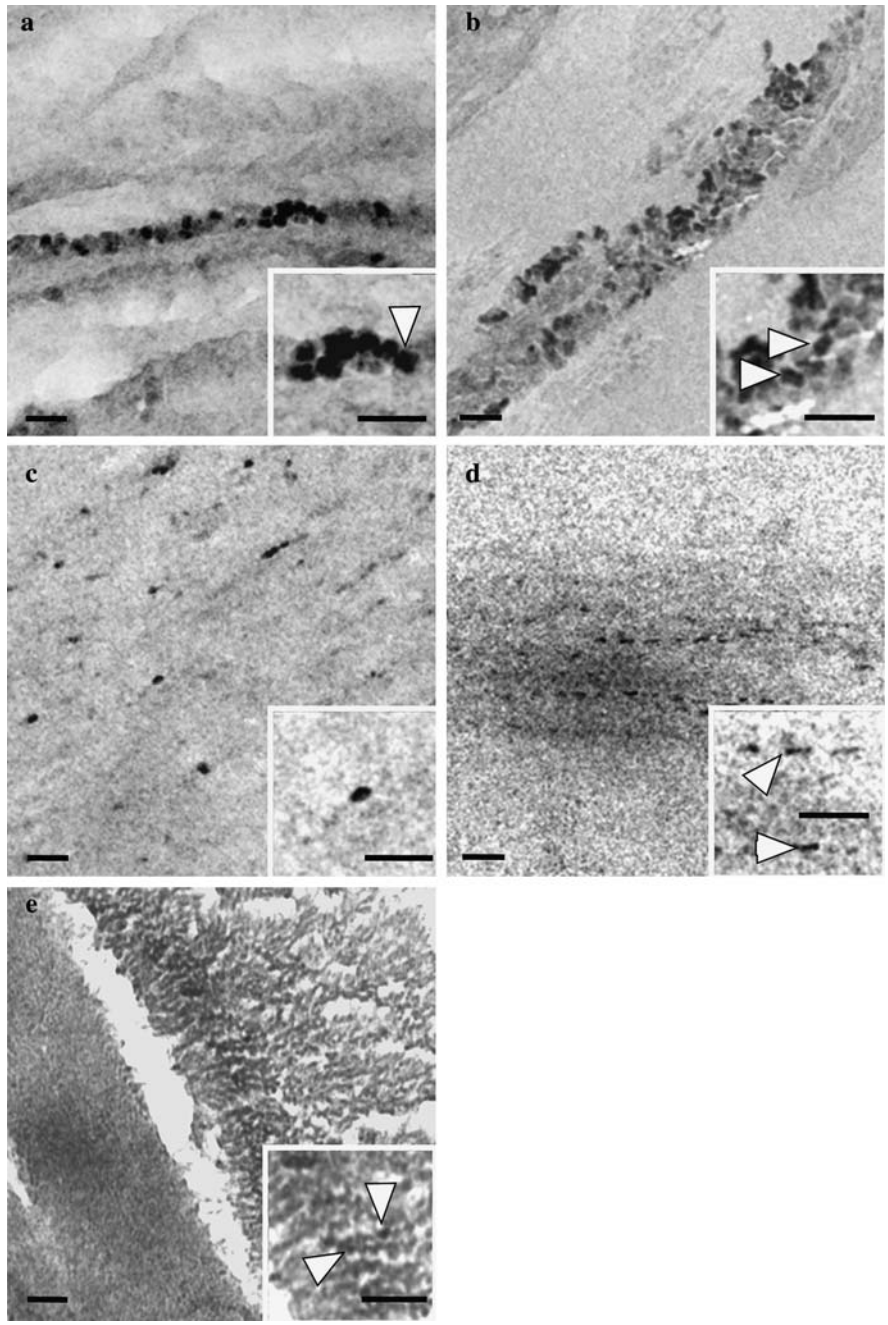

Fig. 4 Bright field images obtained by diffraction contrast imaging for V. ventricosa, H. roretzi, C. intestinalis, M. crux-melitensis, and P. maximowiczii G-layer (**a**–**e**, respectively). Cellulose microfibrils are visualized in black. Each inset is the corresponding magnified cross-section. Individual cellulose microfibrils are indicated by arrowheads. (Bar, 100 nm)

(1998) observed a lattice structure in the cross-sections of *H. papillosa* cellulose by using a uniaxially oriented film. *H. roretzi*, which belongs to the same genus as *H. papillosa*, was observed to have a similar microfibril structure included in the helicoid layers (Fig. 4b). It has recently been suggested that in *C. intestinalis*, which belongs to Cionidae, cellulose synthesis ability was acquired by horizontal transfer from other organisms (Nakashima et al. 2004). As shown in Fig. 4c, the cross-section of *C. intestinalis* microfibrils is smaller than that of *H. roretzi*, which is consistent with the curves of the *R* values at elevated temperatures. In *M. crux-melitensis*, cellulose microfibril cross-sections were observed to form different rectangular faces (Fig. 4d), which were larger than those for the *P. maximowiczii* G-fiber (Fig. 4e) but

thinner than those of *V. ventricosa*. This diffraction contrast image coincided with the *M. crux-melitensis* curve, which has a higher *R* value at 25 °C and exhibits rapid rehydrogenation at approximately 150 °C. This good concurrence in the results demonstrates that the processes occurring during rehydrogenation at elevated temperatures could be reflected in the images of microfibril cross-sections.

Electron microscopy has often been used to measure the microfibril size. Negative staining is widely used for measuring microfibril size because it is a very simple procedure with high resolution. Metal shadowing—the technique with which Preston et al. (1948) obtained the first images of cellulose microfibrils—has also been used for estimating the thickness of microfibrils on the basis of the geometry of the shadow length. More recently, atomic force microscopy (AFM) has also been applied to the characterization of cellulose by means of cantilever scanning, which produces microfibril images with atomic resolution (Baker et al. 1997, 1998). Since the cellulose microfibril is crystalline in nature, X-ray diffractometry has been applied to measure cellulose microfibrils by estimating the crystal width from the diffraction peaks. Very recently, Elazzouzi-Hafraoui et al. (2008) exhibited cross-sectional dimensions evaluated by applying Scherrer's expression from the wide angle X-ray diffractometry. Nuclear magnetic resonance (NMR) is also a useful technique for estimating microfibril dimensions. By separating the signals assigned to cellulose crystallites from those assigned to amorphous material, it has been demonstrated that the lateral dimensions correlated with the size characterized by X-ray diffractometry (Newman 1999).

Very recently, Montanari et al. (2005) succeeded in estimating microfibril size by means of a unique reaction mechanism brought about by TEMPO oxidation, a technique in which only the surface primary OH groups are oxidized. NMR enables the separation of the surface from the crystalline core domain, thereby facilitating the estimation of microfibril dimensions. The values obtained with this unique technique quantitatively corresponded to the microfibril sizes measured from the TEM images. In this study, we used FTIR to characterize the cellulose microfibril structure of several different species in terms of accessibility. The results obtained are consistent with the general assumptions and TEM observations. FTIR analysis in conjunction with rehydrogenation at 25 °C is similar to the TEMPO reaction procedure in that the domain of the surface vs. crystalline core was calculated. The FTIR measurements combined with deuteration/rehydrogenation further enabled us to observe the microfibril shape by means of the OH recovery process at elevated temperatures.

Conclusion

Deuteration/rehydrogenation combined with the FTIR technique was applied to cellulose of various origins in order to characterize each cellulose microfibril. We have shown the possibility that the *R* value at 25 °C correlates with the FWHM of the (200) peak by X-ray diffractometry. It is indicating that the FTIR analysis with rehydrogenation at 25 °C after intracrystalline deuteration could be used to estimate the microfibril dimensions. The OD to OH recovery process at elevated temperature was in good agreement with the cross-section of each microfibril as measured by diffraction contrast. Therefore, the FTIR measurement with the deuteration and rehydrogenation techniques further enabled us to observe the microfibril shape.

Acknowledgments The authors express their grateful appreciation to Dr. H. Ono of the Asahi Kasei Corporation for providing us with several cellulose samples. This study was partially supported by a Grant-in-Aid for Scientific Research (nos. 19208017).

References

Baker AA, Helbert W, Sugiyama J, Miles MJ (1997) High-resolution atomic force microscopy of native *Valonia* cellulose I microcrystals. J Struct Biol 119:129–138. doi:10.1006/jsbi.1997.3866

Baker AA, Helbert W, Sugiyama J, Miles MJ (1998) Surface structure of native cellulose microcrystals by AFM. App Phys A 66:S559–S563

Elazzouzi-Hafraoui S, Nishiyama Y, Putaux JL, Heux L, Dubreuil F, Rochas C (2008) The shape and size distribution of crystalline nanoparticles prepared by acid hydrolysis of native cellulose. Biomacromolecules 9(1):57–65. doi:10.1021/bm700769p

Giddings TH, Brower DL, Staehelin LA (1980) Visualization of particle complexes in the plasma membrane of *Micrasterias denticulata* associated with the formation of cellulose fibrils in primary and secondary cell walls. J Cell Biol 84:327–339. doi:10.1083/jcb.84.2.327

Helbert W, Nishiyama Y, Okano T, Sugiyama J (1998) Molecular imaging of *Halocynthia papillosa* cellulose. J Struct Biol 124:42–50. doi:10.1006/jsbi.1998.4045

Horikawa Y, Sugiyama J (2008) Accessibility and size of *Valonia* cellulose microfibril studied by combined deuteration/rehydrogenation and FTIR technique. Cellulose 15:419–424. doi:10.1007/s10570-007-9187-z

Kim NH, Herth W, Vuong R, Chanzy H (1996) The cellulose system in the cell wall of *Micrasterias*. J Struct Biol 117:195–203. doi:10.1006/jsbi.1996.0083

Kimura S, Laosinchai W, Itoh T, Cui XJ, Linder CR, Brown RM (1999) Immunogold labeling of rosette terminal cellulose-synthesizing complexes in the vascular plant *Vigna angularis*. Plant Cell 11:2075–2085

Koyama M, Sugiyama J, Itoh T (1997) Systematic survey on crystalline features of algal celluloses. Cellulose 4:147–160. doi:10.1023/A:1018427604670

Maréchal Y, Chanzy H (2000) The hydrogen bond network in I_β cellulose as observed by infrared spectrometry. J Mol Struct 523:183–196. doi:10.1016/S0022-2860(99)00389-0

Montanari S, Roumani M, Heux L, Vignon MR (2005) Topochemistry of carboxylated cellulose nanocrystals resulting from TEMPO-mediated oxidation. Macromolecules 38:1665–1671. doi:10.1021/ma048396c

Mueller SC, Brown RM (1980) Evidence for an intramembrane component associated with a cellulose microfibril-synthesizing complex in higher plants. J Cell Biol 84:315–326. doi:10.1083/jcb.84.2.315

Nakashima K, Yamada L, Satou Y, Azuma J, Satoh N (2004) The evolutionary origin of animal cellulose synthase. Dev Genes Evol 214:81–88. doi:10.1007/s00427-003-0379-8

Newman RH (1999) Estimation of the lateral dimensions of cellulose crystallites using ^{13}C NMR signal strengths. Solid State Nucl Mag 15:21–29. doi:10.1016/S0926-2040(99)00043-0

Nishiyama Y, Isogai A, Okano T, Müller M, Chanzy H (1999) Intracrystalline deuteration of native cellulase. Macromolecules 32:2078–2081. doi:10.1021/ma981563m

Preston RD, Nicolai E, Reed R, Millard A (1948) An electron microscope study of cellulose in the wall of *Valonia ventricosa*. Nature 162:665–667. doi:10.1038/162665a0

Revol JF (1982) On the cross-sectional shape of cellulose crystallites in *Valonia ventricosa*. Carbohydr Polym 2:123–134. doi:10.1016/0144-8617(82)90058-3

Ruelle J, Yamamoto H, Thibaut B (2007) Growth stresses and cellulose structural parameters in tension and normal wood from three tropical rainforest angiosperm species. BioRes 2:235–251

Sugiyama J, Harada H, Fujiyoshi Y, Uyeda N (1984) High resolution observations of cellulose microfibrils. Mokuzai Gakkaishi 30:98–99

Sugiyama J, Harada H, Fujiyoshi Y, Uyeda N (1985) Lattice images from ultrathin sections of cellulose microfibrils in the cell wall of *Valonia macrophysa*. Kutz Planta 166:161–168. doi:10.1007/BF00397343

Van Daele Y, Revol JF, Gaill F, Goffinet G (1992) Characterization and supramolecular architecture of the cellulose-protein fibrils in the tunic of the sea peach (*Halocynthia papillosa*, Ascidiacea, Urochordata). Biol Cell 76:87–96. doi:10.1016/0248-4900(92)90198-A

Wada M (2002) Lateral thermal expansion of cellulose I_β and III_I polymorphs. J Polym Sci. Part B Polym Phys 40:1095–1102. doi:10.1002/polb.10166

Washusen R, Evans R (2001) The association between cellulose crystallite width and tension wood occurrence in *Eucalyptus globulus*. IAWA J 22:235–243